New model of crack propagation of aluminium wire bonds in IGBT power modules under low temperature variations

Ayda Halouani, Zoubir Khatir, R. Lallemand, Ali Ibrahim, Nicolas Degrenne

New model of crack propagation of aluminium wire bonds in IGBT power modules under low temperature variations

A. Halouani[a, *], Z. Khatir[a], R. Lallemand[a], A. Ibrahim[a], N. Degrenne[b]

[a] *Gustave Eiffel University, Paris-Saclay University, ENS Paris-Saclay, CNRS, SATIE, 78000 Versailles, France*
[b] *Mitsubishi Electric R&D Centre Europe, 1 Allée de Beaulieu, 35708 Rennes, France*

Abstract

In this paper, a new model of lifetime prediction for wirebond degradation during power cycling in IGBT power module is proposed. This model is based on experimental crack propagation analyses and on a plastic strain empirical law. For the experiments, two power cycling tests in switching mode under high voltage were carried out respectively with temperature swing $\Delta T_j = 30°C$ and $\Delta T_j = 40°C$ and minimal temperature $T_{j,min} = 55°C$. The DUTs and test conditions have been chosen so that only degradations on chip top-side interconnections were observed. The on-state voltage (V_{CE}) was measured during the tests as an indicator of the degradation in the wire and metallization and samples were removed at different aging stages. The removed samples were cross-sectioned in order to observe the crack propagation evolution with cycling. Concerning the plastic strain empirical law, we used results from literature that show the evolution of the plastic strain ($\Delta\varepsilon_{pl}$) with bond-wire contact crack growth. As results, this new lifetime prediction model based on a modified Paris's law for aluminium wire bonds fatigue of IGBTs shows a good fitting of the test results and is used to predict the lifetime. Finally, the lifetime of tested IGBT modules are estimated and used to verify the effectiveness of the proposed model.

1. Introduction

IGBTs are important power semiconductor devices that are widely used in smart grid, household appliances, electric vehicles, and other applications [1]. Due to the mismatch of thermal expansion coefficients between packaging materials, an IGBT module can be subjected to thermal stresses, which eventually lead to the fatigue failure of the package [2]. Many studies have shown that the fatigue of the wire-metallization interface is one of the main failure modes in IGBT modules [3]. After a sufficient number of power cycles, the crack initiates from wire edges even with low stress and continuously propagates [4]. Therefore, research into the fatigue mechanism and lifetime prediction for the wire-metallization interface in IGBTs is crucial to enhancing IGBT reliability.

Although Al wire bond reliability has been a continually evolving subject of research for the last three decades, until now, the lifetime estimation of a wire bond joint has not been thoroughly investigated. Different lifetime models for wire bond have been developed, which includes analytical and physical models [5,6]. Physical lifetime models of wire bond in IGBT packages are divided into four categories: stress, damage, energy-based and strain models. For the first type, the lifetime depends on the stress, mechanical testing frequency (f), and temperature variation (ΔT_j) [7]. For the second type, the lifetime is related to the stress induced by material degradation, cracking, crack propagation, and recrystallization [8,9]. For the lifetime models based on energy depends on the mean temperature (T_m), the power cycling frequency (f), and a coefficient power of f [10]. The lifetime models based on inelastic strain are advantageous to other models because they can accurately represent the strain physical process of materials and illustrate the loading history. Most of the works use the Coffin Manson approach to predict the wire bond lifetime [11,12]. There the plastic strain per thermal cycle ($\Delta\varepsilon_{pl}$) is correlated to the wire bond lifetime N_f, by a coefficient and an exponent [13-15]. In this fatigue law the size of the interface area of crack propagation and the plastic strain evolution with cycling are not taken into account. The Coffin-Manson approach introduces uncertainty in lifetime prediction since the interface area's size and shape depend on the bond tool used, and bond wire diameter

* Corresponding author. ayda.halouani@univ-eiffel.fr

and the plastic strain considered to be constant with cycling. For all these reasons, a modified model of the Paris law, where the cyclic stress intensity factor (ΔK) is replaced by the averaged plastic strain per thermal cycle ($\Delta\varepsilon_{pl}$) is proposed. It permits to predict the lifetime of a wire bond independently from its area size and shape. Also, the plastic strain evolution with cycling could be taken into account. This approach has been proposed in [16] and [17] to determine the lifetime of aluminum heavy wire bond joints.

In this paper, an experimental and theoretical study was carried out. Firstly, power cycling tests in switching mode under high voltage were realized under low temperature swings. Then, a series of cross-sections analyses at different degradation levels are performed to study the crack growth evolution with cycles at the contact interface wire-metallization. Subsequently, an improved strain-based lifetime prediction model based on modified Paris's law for aluminium wire bonds fatigue of IGBTs is proposed. This one is constructed using the experimental observations on crack propagation and results from [16] which gives the variation of $\Delta\varepsilon_{pl}$ with crack growth. Finally, the effectiveness of the proposed model is successfully verified by comparing with experimental aging test results.

2. Experimental procedures

2.1. Tested power module

Commercially available insulated gate bipolar transistor (IGBT) modules (1200V-150A) was chosen in order to study the degradations of Al wires with diameter of 360 µm. The wires were ultrasonically bonded to a metallization layer on Si chips which were soldered onto direct copper bonded (DCB) substrates. The figure 1 gives a photo of a switch cell of a tested module. The tested chip is the IGBT chip. This type of module was chosen because preliminary observations showed that bonding degradations are the only mechanism that occurs in it. Especially, the main degradations occur at the long wires, numbered from 1 to 6 in fig.1. This has also been verified in the tests carried out here. In the following, all the cross-sections were made at the contact of wire#3 (see fig.1) for the crack growth analyses.

2.2. Power cycling in switching mode

IGBT power modules have been tested using power cycling in switching mode. The test bench is described in [18]. Two test campaigns were defined with different ΔTJ stress conditions (30°C and 40°C). We choose to keep the RMS current (IRMS), the duty cycle (k) and heating time (tON) identical for both tests.

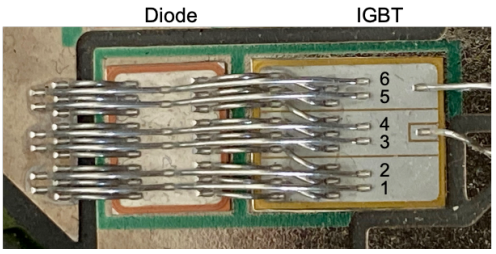

Fig.1. Photo of a switch cell of a tested device.

The adjustment of the ΔT_J was made by the switching losses with different switching frequencies (f_{sw}). Thus, the two tests are defined as follows :

- Test#1 : ΔT_J = 30°C, f_{sw} = 10 kHz,
- Test#2 : ΔT_J = 40°C, f_{sw} = 18 kHz,

and the common conditions were:

- a minimum junction temperature ($T_{j,min}$) set at 55°C using a liquid cooling and a thermoregulator;
- the heating and cooling duration's (t_{ON}/t_{OFF}) were fixed at 40ms/100ms;
- the RMS current was I_{RMS} = 100A;
- and the duty cycle was k = 95%.

During the power cycling tests, the junction temperature was measured using Vce(Tj) as thermosensitive parameter under a small current (100mA), when the power current is off. The T_{jmin} is measured at the end of the cooling period just before the rise of the power current and the T_{jmax} at the end of the heating period, a few hundred microseconds after the falling of the power current. An extrapolation of the Vce(T_{jmax}) is made to correct this small delay for a better approximation of the T_{jmax}.

For each test campaign, six devices were tested on which a single IGBT (Fig. 1) was operated. In both test campaigns, the DUTs were removed at different cycle numbers and degradation levels in order to observe and analyse the crack propagation with aging stage. As a result, these two power cycling tests were not carried out until device failure, but was periodically stopped in order to remove each device from the test bench definitively.

2.3. Cross-sections

Cross-sections of all the tested devices were realized at the wire#3 shown in Fig. 1 and microstructural investigations of aluminium wire and metallization were carried out at metallographically prepared samples.

3. Results and discussion

3.1. Power cycling results

As mentioned above, the aging indicator used to quantify the damage in the wire bonds is the on-state voltage (V_{CE}). This latter is indeed directly impacted by the loss of contact between the wire and the metallization [1]. As a result, table 1 and 2 give the results obtained respectively for test#1 and test#2, where DUTs are referenced from M1 to M6 for test#1 and from M7 to M12 for test#2. These table show the number of cycles undergone by each DUT before its removal and the corresponding level of degradation, given by the relative variation of Vce.

The V_{CE} evolution of each tested device with the cycling is shown in Figs. 2 and 3 respectively for test#1 and test#2. The last V_{CE} measurement for each device (colored big dots in figs.2 and 3), before being removed from the test bench, is an image of the level of degradation at the topside interconnection.

Table 1: Test#1 power cycling results.

DUT ref.	$\Delta V_{CE}/V_{CE}$ (%)	N (Mcycles)
M1	0.24	5
M2	0.40	10
M3	0.44	20
M4	0.57	40
M5	0.62	80
M6	0.46	120

Table 2: Test#2 power cycling results.

DUT ref.	$\Delta V_{CE}/V_{CE}$ (%)	N (Mcycles)
M7	0.27	1
M8	0.42	2
M9	0.65	4
M10	1.12	8
M11	1.68	16
M12	1.62	32

The Vce evolutions in these figures seem fairly reproducible despite the dispersion of measurements. Thus, this may confirm the hypothesis of a similar and quite repeatable degradation in all the tested modules.

These figures show comparable evolutions of Vce whatever the stress ΔTj. A rapid increase at the beginning followed by a relative slowdown during the cycles. Of course, the lower the ΔTj, the earlier the slowdown is observed. This only translates the slightest damage to low stress. For example, for ΔTj=30°C, it is necessary to undergo more than 80Mcycles to observe an increase of only 0.6% in Vce. Whereas after 20Mcycles the Vce reaches an increase of 1.6% in the case of ΔTj=40°C.

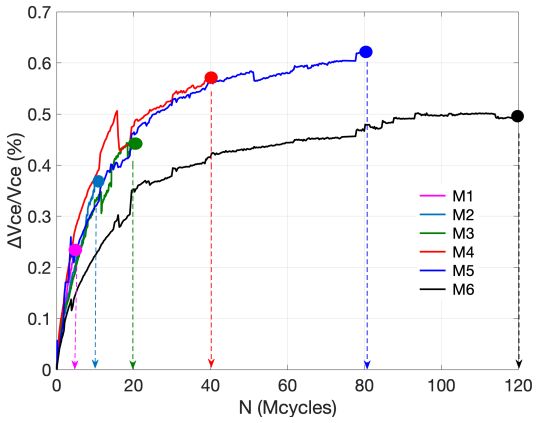

Fig.2. Test#1 – Power cycling results (ΔT_J = 30°C, T_{JMIN} = 55°C, t_{ON}/t_{OFF} = 40ms/100ms, I_{RMS} = 100A, f_{sw} = 10kHz, k = 95%)

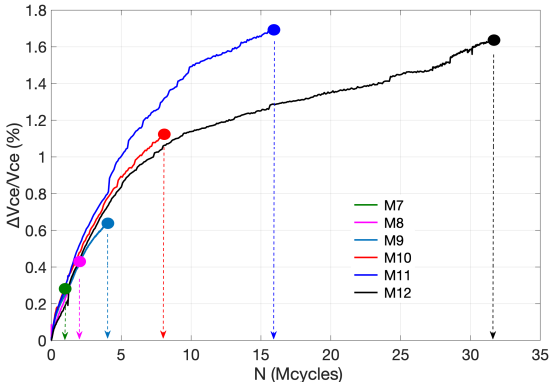

Fig.3. Test#2 – Power cycling results (ΔT_J = 40°C, T_{JMIN} = 55°C, t_{ON}/t_{OFF} = 40ms/100ms, I_{RMS} = 100A, f_{sw} = 18kHz, k = 95%)

3.2. Crack evolution

In the following, the crack length a is defined as the sum of the toe-side and heel-side cracks lengths, excluding any existing pre-crack. The crack ratio (a/l_0) is defined as the crack length over the initial contact length (l_0) (see Fig. 4).

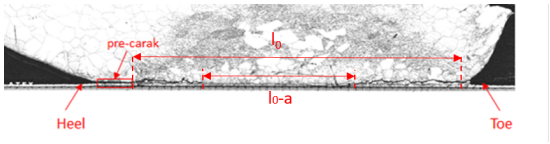

Fig. 4. Interface wire-metallization.

Fig.4 show that crack initiates from the heel and toe sides and continuously propagates along the wire-metallization interface from the edges toward the center. This is because the plastic strain at the corners of the wire-metallization interface is the largest. When

the crack initiates from this place, the plastic strain becomes the largest at the tip of the crack, so the crack will propagate to the center along the wire-metallization interface. Nevertheless, in the process of temperature variation from $55°C$ to $85°C$ (test#1) and to $95°C$ (test#2), the coarsening of aluminum grains will lead to weak points between grains, changing the propagation path of cracks [19]. Therefore, the shape of cracks in solder is irregular, and cracks all propagate near the wire-metallization interface.

Fig. 5 and Fig. 6 shows the evolution of the crack lengths with the number of cycles for test#1 and test#2, green and blue circles represent the crack length calculated on the six DUTs. It can be seen that for both tests that crack-growth rate decreases as the number of power cycling increase. This is because the plastic strain variation decreases when crack length increases.

In fact, the decrease in average plastic strain with increasing crack length is attributed to a reduction in load bearing capacity of the remaining wire-metallization interface. As the crack length increases, the stress required to induce further crack in the remaining bond length is reduced. This trend is consistent with the findings in [20], it was reported a similar pattern in their experiments. It is also similar to the reduction in bond shear strength that occurs with increasing crack growth, as reported in [21].

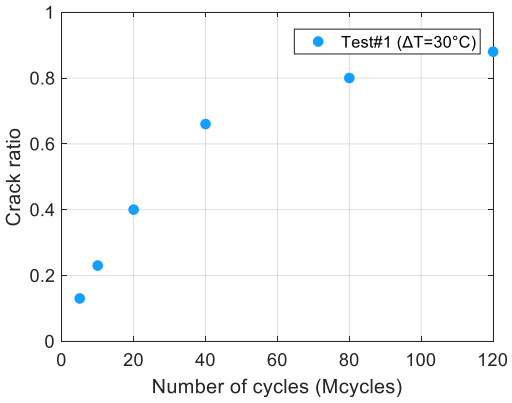

Fig. 5. Experimental Crack growth for test#1 at wire#3.

Despite the low value of Vce (less than 5%) shown in Fig.2 and Fig.3, the crack ratio reaches 0.9 at 120 Mcycles and 32 Mcycles for test#1 and test#2 respectively. In fact, as mentioned above, the micro-sections are performed at wire#3 where the higher thermal stress is expected and is probably the most damaged wire.

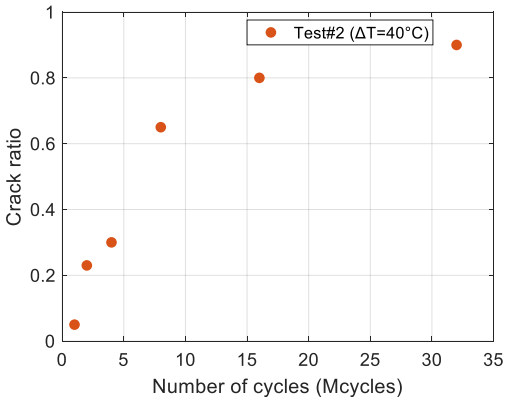

Fig. 6. Experimental Crack growth for test#2 at wire#3.

4. Crack propagation model

As mentioned above, the crack-growth rate for both power cycling tests and the plastic strain variation ($\Delta\epsilon_{pl}$) share the same tendency. They continuously decrease with cycling. Based on this instigation, in [16], a modified Paris law has been investigated considering the fatigue crack, which propagates through the interface area for aluminum heavy wire bond joints, here, that stress intensity is replaced by plastic strain variation:

$$\frac{da}{dN} = c_1\left(\Delta\epsilon_{pl}\right)^{c_2} \tag{1}$$

where a is the crack length, N is the number of cycles, $\Delta\epsilon_{pl}$ is the plastic strain variation per cycle, c_1 and c_2 are two empirical parameters. FEM simulations performed in [16] have made it possible to draw the evolution of plastic strain change with interface area, the interface has an ellipse geometry of semi-axes l_x and l_y, where the value of l_x is always double in length the value of l_y even during crack propagation (see ellipse graphic in Fig. 7).

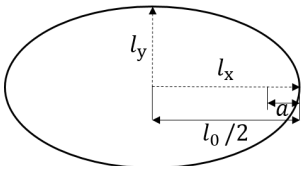

Fig. 7. Elliptic form of the interface area.

The plastic strain variation has been evaluated for 300 µm wire of IGBT module at different temperatures variation (75°C and 105°C), black and blue curves respectively in Fig.8. A strong dependency on geometry as well as temperature was observed. Moreover, with decreasing interface area

(increasing crack area respectively), the plastic strain variation reduces, so that crack growth is slower for smaller interface areas.

In this paper, the evolution tendency of $\Delta\varepsilon_{pl}$ is considered to be the same for $\Delta T = 30°C$ and $\Delta T = 40°C$. The initial value of $\Delta\varepsilon_{pl_0}$ for $\Delta T = 30°C$ and $\Delta T = 40°C$ are from [22] (see Fig. 8).

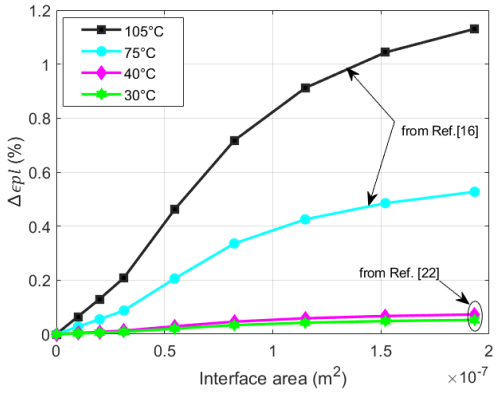

Fig. 8. Plastic strain change with interface area.

Based on the assumption ($l_x = 2l_y$), the evolution of plastic strain change with crack length is plotted in Fig. 9 (red curve for $\Delta T = 30°C$). An approximation of this (red) curve was made, (dotted red curve in Fig.9) represents the $\Delta\epsilon_{pl}$ approximation given by equation 2 (with $\alpha = 3$):

$$\Delta\varepsilon_{pl} = \frac{\Delta\varepsilon_{pl_0}}{\cosh(\alpha\tau)}\ ;\ \alpha = cte\ ;\ \tau = \frac{a}{l_0} \qquad (2)$$

which gives (with the assumption of $c_2 \approx 1$):

$$\tau = 1/\alpha\left(asinh\left(N/k\Delta T_j\right)\right) \qquad (3)$$

where a corresponds to the crack length, N is the number of cycles, α constant that does not depend on ΔT_j, and k a constant depending on the ΔT_j. The evolution of the crack with the cycling for this expression is presented in Fig. 10 and 11. The coefficients for both tests are $k_1 = 14$, $c_1 = 1.6.10^{-4}$ for $\Delta T = 30°C$ and $k_2 = 3.2$, $c_1 = 5.10^{-4}$ for $\Delta T = 40°C$. Moreover, the number of cycles to failure (N_f) was determined, it was found for $N_f \approx 180.10^6$cycles for $\Delta T = 30°C$ (Test#1) and $N_f \approx 42.10^6$ cycles for $\Delta T = 40°C$ (Test#2).

Results in Fig. 9 show that $\Delta\epsilon_{pl}$ keeps a high value at the crack initiation stage then it decreases continuously with crack propagation. This is due to the microscopic mechanism between crack initiation and crack propagation. The dislocations and slips of the metal lattice in aluminum are the reasons for crack initiation. Dislocations would continually combine to develop micro-cracks [14]. Nevertheless, with periodic thermal stress, the reasons for crack propagation open and close continually at the tip of the crack.

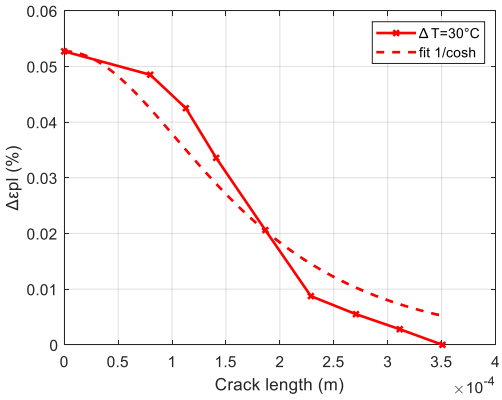

Fig. 9. Plastic strain change with crack length (red curve) and fitted curve (dotted lines).

Due to the difference of mechanism upon crack propagation, the variation in $\Delta\epsilon_{pl}$ allows to better characterize the processes of crack growth at the wire-metallization interface.

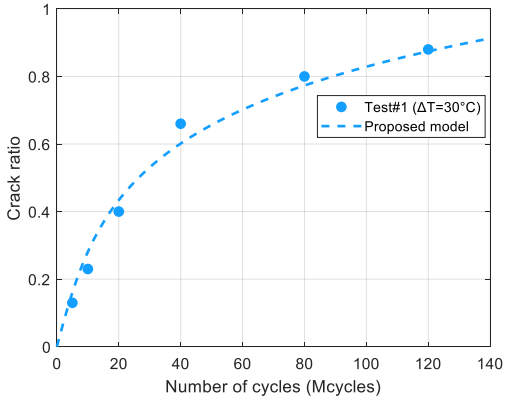

Fig. 10. Evolution of the crack with the cycling for "test#1" (blue circles) and proposed model (blue dotted line).

5. Validation of the proposed model

In order to verify the validity of the lifetime model proposed in this paper, additional power cycling tests (test#3 and test#4) with the same conditions (test #1 and test#2) respectively, were conducted. However, those tests were performed for longer time in order to determine the number of cycles

to failure (N_f).

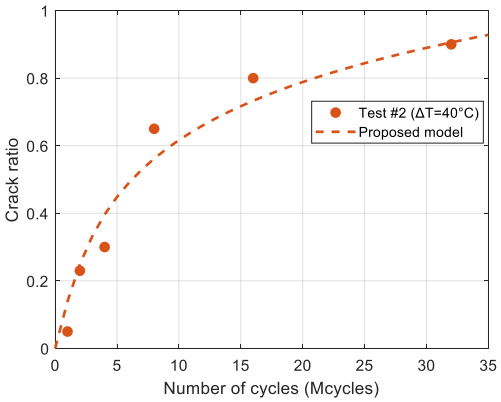

Fig. 11. Evolution of the crack with the cycling for "test#2" (orange circles) and proposed model (orange dotted line).

Concerning the test#3 ($\Delta T_J = 30°C$, $T_{JMIN} = 55°C$, $t_{ON}/t_{OFF} = 40ms/100ms$, $I_{RMS} = 100A$, $f_{sw} = 10kHz$, $k = 95\%$), despite the large number of cycles carried out, the voltage (Vce) always remains very low (around 1.6 %) because of the low temperature variation. Due to the huge time it required this test, it was stopped.

Here, only the results of test#4 ($\Delta T_J = 40°C$, $T_{JMIN} = 55°C$, $t_{ON}/t_{OFF} = 40ms/100ms$, $I_{RMS} = 100A$, $f_{sw} = 18kHz$, $k = 95\%$) were presented (see dotted lines in Fig. 12). It can be seen the main assumption that all DUTs age in the same way under the identical stress conditions seems quite well verified. In addition, test#4 results show that V_{CE} gradually increases until an apparent saturation around 1.75% then the V_{CE} undergoes a sharp and stepped increase, representative of the bond-wire lift-off. Considering these results, the number of cycles to failure (N_f) is around 40 Mcycles.

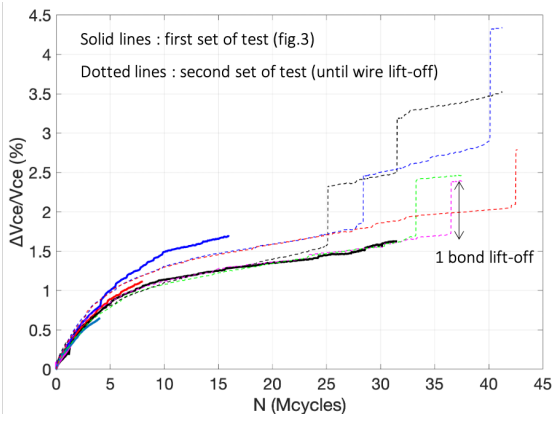

Fig. 12. Power cycling results for $\Delta T_j = 40°C$ (solid lines, Test#2) and (dotted lines, Test#4)

Based on these results, the assumption of $\Delta\epsilon_{pl}$ evolution on inverse hyperbolic cosine have been proven to be correct in thick wire bonds for IGBT module under low temperature variation in this paper.

5. Conclusions

An improved strain-based lifetime prediction model based on modified Paris's law for aluminium wire bond degradation of IGBT power module under low temperature variation is proposed in this paper. The model is based on a combination of experimental crack propagation results and on a plastic strain empirical law. The experimental crack propagation results show that crack-growth rate continuously decrease with cycling. For the plastic strain empirical law, results from literature that show the evolution of the plastic strain ($\Delta\epsilon_{pl}$) with bond-wire contact crack growth were used. Finally, the lifetime of tested IGBT modules were estimated. The predicted results show good agreement with the experimental results, which verified the accuracy of the proposed lifetime model.

References

[1] N. Dornic *et al.* Analysis of the aging mechanism occurring at the bond-wire contact of IGBT power devices during power cycling. Microelectronics Reliability, 2020, vol. 114.

[2] K. Sasaki *et al.* Thermal and structural simulation techniques for estimating fatigue life of an IGBT module. 20th International Symposium on Power Semiconductor Devices and IC's. IEEE, 2008. p. 181-184.

[3] J.-M. Thebaud *et al.* Strategy for designing accelerated aging tests to evaluate IGBT power modules lifetime in real operation mode. IEEE Trans. on components and packaging technologies, 2003, vol. 26, nº2, p. 429-438.

[4] A. Morozumi *et al.* Reliability of power cycling for IGBT power semiconductor modules. IEEE Trans. on Industry Applications, 2003, vol. 39, no 3, p. 665-671.

[5] A. Morozumi *et al.* Reliability of power cycling for IGBT power semiconductor modules. IEEE Transactions on Industry Applications, 2003, vol. 39, no 3, p. 665-671.

[6] X. WU *et al.* A physical lifetime prediction methodology for IGBT module by explicit emulation of solder layer degradation. Microelectronics Reliability, 2021, vol. 127, p. 114384.

[7] L. Yang *et al.* Physics-of-failure lifetime prediction models for wire bond interconnects in power electronic modules. IEEE Transactions on Device and Materials Reliability, 2012, vol. 13, no 1, p. 9-17.

[8] B. Czerny *et al.* Interface reliability and lifetime prediction of heavy aluminum wire bonds. Microelectronics Reliability 58 (2016): 65-72.

[9] L. Yang et al. A time-domain physics-of-failure model for the lifetime prediction of wire bond interconnects.

Microelectronics Reliability 51.9-11 (2011): 1882-1886.
[10] H. Huang *et al.* A lifetime estimation technique for voltage source inverters. IEEE Transactions on Power Electronics 28.8 (2012): 4113-4119.
[11] X. Yang *et al.* "Lifetime prediction of IGBT modules in suspension choppers of medium/low-speed maglev train using an energy-based approach." IEEE Transactions on Power Electronics 34.1 (2018): 738-747.
[12] G. Khatibi *et al.* Accelerated mechanical fatigue testing and lifetime of interconnects in microelectronics. Procedia Engineering 2.1 (2010): 511-519.
[13] R. Dudek *et al.* Failure Prediction and Analysis of an IGBT Module for Industrial Applications Subjected to Passive and Power Cycling," 2023 24th International Conference on Thermal, Mechanical and Multi-Physics Simulation and Experiments in Microelectronics and Microsystems (EuroSimE), Graz, Austria, 2023, pp. 1-11, doi: 10.1109/EuroSimE56861.2023.10100806.
[14] J. Luo *et al.* Research on Igbt Bonding Wires Crack Propagation at the Macro and Micro Scales. IEEE Access, 2021, vol. 9, p. 106270-106282.
[15] G. Zeng *et al.* Power cycling results of high power IGBT modules close to 50 Hz heating process. In: 2019 21st European Conference on Power Electronics and Applications (EPE'19 ECCE Europe). IEEE, 2019. p. 1-10.
[16] A. Grams *et al.* A geometry-independent lifetime modelling method for aluminum heavy wire bond joints. 2015 16th Intern. Conf. on Thermal, Mechanical and Multi-Physics Simulation and Experiments in Microelectronics and Microsystems. IEEE, 2015. p. 1-6.
[17] A. Grams *et al*., Modelling the lifetime of aluminum heavy wire bond joints with a crack propagation law. In : 2014 15th International Conference on Thermal, Mechanical and Mulit-Physics Simulation and Experiments in Microelectronics and Microsystems (EuroSimE). IEEE, 2014. p. 1-6.
[18] A. Ibrahim *et al.*, Condition monitoring and evaluation of Ron degradation during power cycling of SiC-Mosfets power modules, International Conference on Integrated Power Electronics Systems (CIPS), Berlin, 2022.
[19] A. Halouani *et al*., An EBSD Study of Fatigue Crack Propagation in Bonded Aluminum Wires Cycled from 55°C to 85°C. J. Electron. Mater. 51, 7353–7365 (2022). https://doi.org/10.1007/s11664-022-09937-5
[20] A. Grams *et al*., Modelling the lifetime of aluminum heavy wire bond joints with a crack propagation law. In: 2014 15th International Conference on Thermal, Mechanical and Mulit-Physics Simulation and Experiments in Microelectronics and Microsystems (EuroSimE). IEEE, 2014. p. 1-6.
[21] K. Nwanoro *et al*., Advantages of the extended finite element method for the analysis of crack propagation in power modules. Power Electronic Devices and Components, 2023, vol. 4, p. 100027.
[22] N. Dornic *et al.,* Stress-based model for lifetime estimation of bond wire contacts using power cycling tests and finite-element modelling, IEEE Journal of Emerging and Selected Topics in Power Electronics, vol. 7.3, 2019, p. 1659-1667.